Journal of Materials Chemistry C

Accepted Manuscript

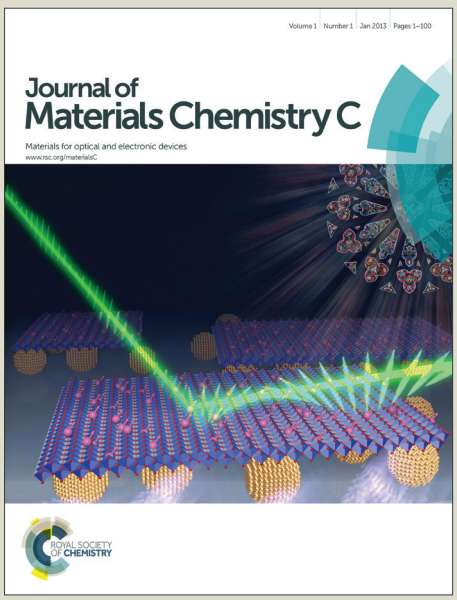

ROYAL SOCIETY OF CHEMISTRY

www.rsc.org/materialsC

Noncentrosymmetric Chalcohalide $NaBa_4Ge_3S_{10}Cl$ with Large Band Gap and IR NLO Response

Kai Feng,[a,b,c] Lei Kang,[a,b,c] Zheshuai Lin,[a,b] Jiyong Yao,[a,b,*] and Yicheng Wu[a,b]

By introducing the highly-electronegative halide anion into chalcogenides, one novel chalcohalide, $NaBa_4Ge_3S_{10}Cl$, has been synthesized by conventional high temperature solid–state method. It crystallizes in a new structure type of space group $P6_3$ with a = 9.7653(2) Å, c = 12.0581(3) Å and Z = 2. The fundamental unit is the unique $[Ge_3S_9]$ ring comprised of three GeS_4 tetrahedra via sharing corner S atoms. The $[Ge_3S_9]$ rings are arranged to form pseudo layers, which are stacked through Na-Cl-Ba chains to build up the structure. The macroscopic packing of these $[Ge_3S_9]$ rings provides the material moderate NLO response at 2090 nm fundamental light. Furthermore, UV-vis-IR spectroscopy shows that $NaBa_4Ge_3S_{10}Cl$ has a very large band gap of 3.49 eV, which is very beneficial to increase the laser damage threshold and avoid the two-photon absorption problem of the conventional near IR laser pumping sources.

[a] *Center for Crystal Research and Development, Technical Institute of Physics and Chemistry, Chinese Academy of Sciences, Beijing 100190, China,*

[b] *Key Laboratory of Functional Crystals and Laser Technology, Technical Institute of Physics and Chemistry, Chinese Academy of Sciences, Beijing 100190, China,*

[c] *University of Chinese Academy of Sciences, Beijing 100049, China*

†Electronic supplementary information (ESI) available: Crystallographic data in CIF format for $NaBa_4Ge_3S_{10}Cl$

Introduction

Mid-far IR lasers have important civil and military applications. So far, the nonlinear optical (NLO) method is an important way to generate mid-far IR lasers.[1, 2] For decades, the $AgGaQ_2$ (Q = S, Se)[3,4] and $ZnGeP_2$[5] crystals have been the benchmark IR NLO materials. These chalcopyrite type crystals possess advantages including large NLO coefficients[6,7] and wide transparent regions.[4-6] However, they have serious drawbacks in properties. For example, $AgGaQ_2$ has low laser damage threshold and $AgGaSe_2$ is non-phase matchable at 1 μm, while $ZnGeP_2$ exhibits strong two-photon absorption (TPA) of the conventional 1 μm or 1.55 μm pumping laser.[8]

The search for new IR NLO crystals with better overall properties is very active nowadays.[9-19] Among the requirements for a good IR NLO material, increasing the laser damage threshold and avoiding TPA of the conventional near IR pumping sources may be the two most demanding ones. An effective way to achieve these goals is to enlarge the band gap by incorporating alkali or alkaline-earth metal. This structural design strategy has led to discovery of several wide-gap alkali metal- or alkaline-earth metal-containing chalcogenide IR NLO materials, including the $LiMQ_2$ (M = Ga, In; Q = S, Se)[20-22] $BaGa_4Q_7$,[23-25] $Li_2Ga_2GeS_6$,[26] $LiGaGe_2Se_6$,[27] $Li_2In_2SiQ_6$,[28] $BaGa_2GeQ_6$[29] materials, some of which are very promising for practical applications.

On the other hand, some halides have also been investigated as IR NLO materials, such as $CsGeX_3$ (X = Cl, Br),[30, 31] SbF_3,[32] $Cs_2Hg_3I_8$,[33] $HgBr_2$,[34] $NaSb_3F_{10}$.[35] Halide IR NLO materials usually possess very large band gaps (3.3, 4.3, 5.0 eV for $HgBr_2$, SbF_3 and $NaSb_3F_{10}$, respectively)[32,34,35] and high laser damage threshold (1.3 and 0.3 GW/cm^2 for $NaSb_3F_{10}$ and $HgBr_2$, respectively),[34,35] but their NLO response is usually much smaller than those of chalcogenides. For example, $HgBr_2$, exhibiting the largest second harmonic generation (SHG) effect among them, has a SHG effect only about 10 times that of KDP (d = 0.39 pm/V).[34] Such values are unfavorable for application. If we could combine the advantage of chalcogenides (large NLO response) with that of halides (large band gap and laser damage threshold) into one compound, we may obtain IR NLO materials with the advantages of both kinds of materials.

Actually, mixed anions compounds, including the *Ln*FeO*Pn* (*Ln* = rare-earth; *Pn* = P, As)[36-38] superconductors, and the LaCuOQ[39] *p*-type transparent conductors, have received intensive investigation. An interesting structural feature in these compounds is that if different cations are involved, a highly electronegative element (e.g., O, F) tends to form strong ionic bonding with a highly electropositive one (e.g., alkali metal), whereas a less electronegative element (e.g., P, As, S, Se, Te) tends to form a stable covalent bonding with a less electropositive one (e.g., *p*-block element). The cooperative interactions of building units with different bonding nature and functions bring the materials fascinating properties. Thus the covalent M–Q (M = *p* block element, Q = chalcogen) framework, which is helpful to generate large NLO response, can be compatibly packed together with the ionic-bonded A–X (A = alkali or alkaline

-earth metal, X = halide) framework, which is helpful to increase the band gap.

In view of the structural stability and property, the anion-mixed chalcohalides are very promising to become a new class of IR NLO materials with desired properties. The study of IR NLO chalcohalides is very limited compared with those in chalcogenides and halides.[40-44] In this work, we investigated the A–Ba–M–Q–X (A = Na, K; M = Ge, Sn; Q = chalcogen; X = halide) system and found one new non-centrosymmetric compound $NaBa_4Ge_3S_{10}Cl$. It possesses unique [Ge_3S_9] rings, moderate NLO response and a very large band gap of 3.49 eV. Such large band gap is very beneficial for increasing the laser damage threshold and avoiding the TPA problem of the conventional 1μm laser pumping sources.

Experimental

Single–crystal Growth

The following reagents were used as obtained: BaS (Sinopharm Chemical Reagent Co., Ltd., 99.9%), Ge (Sinopharm Chemical Reagent Co., Ltd., 99.99%), S (Sinopharm Chemical Reagent Co., Ltd., 99.9%) and NaCl (Sinopharm Chemical Reagent Co., Ltd., 99%). GeS_2 was synthesized by high temperature reaction of elements in sealed silica tubes evacuated to 10^{-3} Pa.

A mixture of BaS, GeS_2 and NaCl with molar ratio of 1:1:1 were ground and loaded into a fused–silica tube under an Ar atmosphere in a glovebox, which was

sealed under 10^{-3} Pa atmosphere and then placed in a computer–controlled furnace. The sample was heated to 1123 K in 20 h and kept at that temperature for 48 h, then cooled at a slow rate of 4 K/h to 673 K, and finally cooled to room temperature. The produced crystals were manually selected for structure characterization. Analyses of the crystals with an EDX–equipped Hitachi S–4800 SEM showed the presence of Ba:Na:Ge:S:Cl in the approximate molar ratio of 20.7:5.5:16.2:51.5:6.1.

Solid–state Synthesis

Polycrystalline sample of the compound was synthesized by solid–state reaction technique. A mixture of BaS, GeS_2 and NaCl according to the stoichiometric ratio were ground and loaded into a fused silica tube under an Ar atmosphere in a glovebox, which was sealed under 10^{-3} Pa atmosphere and then placed in a computer–controlled furnace. The sample was heated to 1223 K in 20 h, kept at that temperature for 48 h, and then the furnace was turned off.

X–ray powder diffraction analysis of the powder sample was performed at room temperature in the angular range of 2θ = 10–70º with a scan step width of 0.02º and a fixed counting time of 1 s/step using an automated Bruker D8 X–ray diffractometer equipped with a diffracted monochromator set for Cu K_α (λ = 1.5418 Å) radiation.

Figure 1 shows XRD pattern of the polycrystalline sample of $NaBa_4Ge_3S_{10}Cl$ along with the calculated one on the basis of the single crystal data. The pattern of the sample is in good agreement with the calculated one. In addition, efforts to synthesize

analogues with other IA and IVA elements in the form of either single crystals or polycrystalline samples were unsuccessful.

Structure Determination

Single–crystal X–ray diffraction data was collected with the use of graphite–monochromatized Mo K_α (λ = 0.71073 Å) at 293 K on a Rigaku AFC10 diffractometer equipped with a Saturn CCD detector. The collection of the intensity data, cell refinement and data reduction were carried out with the use of the program Crystalclear.[45] Face–indexed absorption corrections were performed numerically with the use of the program XPREP.[46]

The structure was solved with the direct methods program SHELXS and refined with the least–squares program SHELXL of the SHELXTL.PC suite of programs.[46] In the situation that elements next to each other in the periodic table are involved, the assignments of atoms are based on the bonding characteristics and bond valence sums calculations. Considering the bonding characteristics in mixed anion/mixed cation compounds, in $NaBa_4Ge_3S_{10}Cl$, all anions connected to the Ge atoms are assigned as S atoms and those connected to Na and Ba only are assigned as Cl atoms. The final refinement included anisotropic displacement parameters and a secondary extinction correction. The program STRUCTURE TIDY[47] was then employed to standardize the atomic coordinates. Additional experimental details are given in Table 1 and selected metrical data are given in Table 2. Further information may be found in Supporting

Information.

Diffuse Reflectance Spectroscopy

A Cary 5000 UV–vis–NIR spectrophotometer with a diffuse reflectance accessory was used to measure the spectrum of $NaBa_4Ge_3S_{10}Cl$ in the range of 300 nm (4.13 eV) to 2100 nm (0.59 eV).

SHG Measurements

The optical SHG response of $NaBa_4Ge_3S_{10}Cl$ was measured by means of the Kurtz–Perry method.[48] The fundamental light is the 2090 nm light generated with a Q–switched Ho:Tm:Cr:YAG laser. The particle size of the sample is 80–100μm. Microcrystalline $AgGaS_2$ of similar particle size served as a reference.

First-principles Calculations

The first-principles calculations at the atomic level for the $NaBa_4Ge_3S_{10}Cl$ crystal, including the band structure, total/partial density of states (DOS/PDOS) and optical properties (SHG effect), are performed by the plane-wave pseudopotential method[49] implemented in the CASTEP[50] program based on density functional theory (DFT).[51] The ion-electron interactions are modeled by the optimized norm-conserving

pseudopotentials[52] of the Kleinman-Bylander form[53] for all constituent elements. In this model, Na $2s^2 2p^6 3s$, Ba $5s^2 5p^6 6s^2$, Ge $4s^2 4p^2$, S $3s^2 3p^4$, and Cl $3s^2 3p^5$ electrons are treated as the valence electrons, respectively. The kinetic energy cutoff of 900 eV and Monkhorst-Pack *k*-point meshes[54] spanning less than 0.04/Å^3 in the Brillouin zone are chosen to ensure the present purposes to be sufficiently accurate.

Result and discussion

Crystal Structure

$NaBa_4Ge_3S_{10}Cl$ crystallizes in a novel structure type of space group $P6_3$ of hexagonal system. The asymmetric unit contains two crystallographically independent Ba atoms, one independent Na atom, one independent Ge atom, four independent S atoms and one independent Cl atom. Na and Cl atoms are at Wyckoff sites 2*a*, Ba2 and S4 atoms are at Wyckoff sites 2*b*, while others are all at general position 6*c*. Considering no metal–metal bond and S–S bond in the structure, the oxidation states of 1+, 2+, 4+, 2– and 1– can be attributed to Na, Ba, Ge, S and Cl, respectively.

As shown in Figure 2, in $NaBa_4Ge_3S_{10}Cl$, each Ge atom is connected by four S atoms in distorted tetrahedral geometry and three such GeS_4 tetrahedra are further linked by sharing corner S atoms to generate the isolated $[Ge_3S_9]$ ring. It is interesting to note the space group $P6_3$ of $NaBa_4Ge_3S_{10}Cl$ is both chiral and polar. The polarity is demonstrated in the connectivity of a single $[Ge_3S_9]$ ring as the three Ge−S2 bonds are all pointed to almost the same direction parallel to the *c* axis. However, the two

$[Ge_3S_9]$ rings in a unit cell are related by the 6_3 screw axis along the *c* axis. As a result, the Ge−S1 and Ge−S3 bonds between the two $[Ge_3S_9]$ rings are rotated by about 60°, demonstrating the chirality of the structure (Figure 2). For the macroscopic packing of these $[Ge_3S_9]$ rings, they are arranged in the same orientation to form a pseudo-layer parallel to the *ab* plane, in which each Na atom is linked by three $[Ge_3S_9]$ rings and each $[Ge_3S_9]$ ring is also linked by three Na atoms (Figure 3A). For two adjacent such pseudo layers, the orientations of the $[Ge_3S_9]$ rings are rotated by 60°. As shown in Figure 3B, Cl atoms are linked by three Ba1 atoms and two Na atoms to generate a bicapped triangular pyramid, which is further linked by sharing Na atoms to form a one-dimensional chain. The pseudo layers of $[Ge_3S_9]$ rings are stacked through the one-dimensional chains to build up the structure with other Ba2 and S4 atoms occupying the interspaces.

Figures 4A and 4B illustrate the coordination environment of all cations. Ge atoms are coordinated to four S atoms to form tetrahedra with Ge–S distances from 2.149(4) to 2.265(3) Å, which are usual in $BaGa_2GeS_6$ (2.212(1) to 2.239(1) Å)[29] and $LiIn_2GeS_6$ (2.180(1) to 2.197(1) Å).[28] 5–fold Na atom is connected with three S atoms and two Cl atoms to generate trigonal bipyramid with two Cl atoms as apex. The Na–S bond length is 2.820(3) Å, comparable to those in $LiNaAs_2S_4$ (2.740(1) to 2.941(1) Å)[10] and $NaMo_6S_8$ (2.608(1) to 3.150(1) Å),[55] and Na–Cl bond lengths change from 3.004(17) to 3.025(17) Å, a little longer than those of $Na_2Ti_3Cl_8$ (2.791(1) to 2.879(1) Å)[56] and NaCl (2.829(1) Å).[57] Ba1 atom is coordinated to seven S atoms and one Cl atoms to generate distorted rectangular prism while Ba2 atom is linked by

seven S atoms to form mono-capped trigonal prism. Ba–S bond lengths range from 2.991(2) to 3.561(4) Å, resembling those of Ba_2AgInS_4 (3.128(2) to 3.314(2) Å)[58] and Ba_3PrInS_6 (3.171(1) to 3.335(1) Å),[59] and Ba–Cl distance is 2.994(1) Å, a bit shorter than those in $Ba_8Eu_7Cl_{34}$ (3.090(1) to 3.563(1) Å)[60] and Ba_2GdCl_7 (3.091(1) to 3.328(1) Å).[61]

The $[Ge_3S_9]$ ring is also seen in the structure of $EuGeS_3$,[62] but $EuGeS_3$ crystallizes in the centrosymmetric space group $P\bar{1}$ and the two $[Ge_3S_9]$ rings in a unit cell are related via an inversion center. In comparison, $NaBa_4Ge_3S_{10}Cl$ crystallizes in the non-centrosymmetric polar $P6_3$ space group and the two $[Ge_3S_9]$ rings in a unit cell are not related via an inversion center but the 6_3 screw axis. In addition, the GeS_4 tetrahedra have also exhibited other kinds of connectivity in other compounds. For example, in Tl_4GeS_4[63] and $LaCa_2GeS_4Cl_3$,[40] the GeS_4 tetrahedra are isolated from each other; in $Rb_2Ge_2S_5$[64] and $RbTaGeS_5$,[65] two GeS_4 tetrahedra form $[Ge_2S_6]$ anionic groups by sharing edge; while the structural motif of $Na_6Ge_2S_7$[66] is $[Ge_2S_7]$ anion also built from two GeS_4 tetrahedra via sharing corner S atom. In more complex situations, four GeS_4 tetrahedra are connected by sharing corner S atoms to form $[Ge_4S_9]$ anion groups in $Na_2Ge_2S_5$[67] and $K_2Ge_2S_5$[64] and the GeS_4 tetrahedra are linked by sharing corner S atoms to generate one-dimensional chains in Na_2GeS_3.[68]

SHG measurement

The SHG signal intensity of $NaBa_4Ge_3S_{10}Cl$ with the 2090 nm laser as fundamental wavelength was about one third of that of $AgGaS_2$ with similar particle size. According to anionic group theory,[69-71] which is very successful in explaining the NLO properties of materials, the macroscopic SHG effect is the summation of microscopic anion groups. If the anion groups are arranged parallelly, the SHG response will be strong. As discussed in the structure part, the basic microscopic NLO-active functional units, i.e. the GeS_4 tetrahedra, are connected via corner-sharing to generate $[Ge_3S_9]$ rings, which are then joined by Na cation to form pseudo layers. The polarity and chirality of the structure have significant influence on the packing of the $[Ge_3S_9]$ rings: In a single pseudo layer, the $[Ge_3S_9]$ rings are aligned in almost the same direction and should be beneficial to generate strong NLO response. However, two adjacent such pseudo layers are related by the 6_3 screw axis, the orientations of the $[Ge_3S_9]$ rings are rotated by 60^o and only the polar arrangement of the Ge−S2 bonds is maintained, which reduces the overall macroscopic NLO properties. A similar structural feature was observed in the $K_2Al_2B_2O_7$[72, 73] borates. As a result, $NaBa_4Ge_3S_{10}Cl$ provides moderate NLO response, i.e., one third of $AgGaS_2$. Considering the large NLO coefficient of $AgGaS_2$ (d_{36} = 14.1 pm/V), although such NLO response of $NaBa_4Ge_3S_{10}Cl$ is not very large in chalcogenide NLO materials, it is still larger than those of most oxides and halides, such as β-BaB_2O_4 (d_{22}(1064nm) = 2.2 pm/V),[74] LiB_3O_5 (d_{32}(1064nm) = 0.85 pm/V),[75] $CsGeCl_3$ (d_{15}(cal.) = 1.1 pm/V)[16] and $NaSb_3F_{10}$ (d_{33}(cal.) = –0.83 pm/V).[16]

Experimental Band Gap

Figure 5 shows the diffuse reflectance spectrum of $NaBa_4Ge_3S_{10}Cl$. The absorption edge of $NaBa_4Ge_3S_{10}Cl$ is 355 nm, and consequently the band gap of 3.49 eV is deduced by the straightforward extrapolation method.[76] This value is much larger than those of most chalcogenide IR NLO materials (2.8, 1.8 eV for $AgGaS_2$ and $AgGaSe_2$)[7] and comparable to those of halide (3.1, 3.3 eV for $CsGeCl_3$, $HgBr_2$),[30,34] which clearly demonstrates that the incorporation of the halide ion into chalcogenides can effectively increase the band gap. Such phenomena may be explained via the "dimensional reduction" concept also exhibiting in other series of compounds:[77-82] A large band gap may help to increase the laser damage threshold of the material and avoid the TPA problem of the conventional near IR laser pumping sources (Nd: YAG 1064nm laser, for example).

First-Principles Calculation

The electronic band structure of $NaBa_4Ge_3S_{10}Cl$ calculated by local density approximation (LDA)[83] method in the unit cell is plotted along the symmetry lines in Figure 6A. The corresponding PDOS is displayed in Figure 6B. It is clear that the energy region below –10 eV is mainly composed of the isolated inner orbitals of Na (2s) (2p), Ba (5s) (5p), S (3s) and Cl (3s), which are strongly localized deep in the valence band (VB) and have a negligible influence on the IR optical properties.[84] The top of the VB is mainly occupied by the *p* orbitals of Ge (3p), S (3p) and Cl (3p), and

the bottom of conduction band (CB) is mainly contributed by the orbitals of Ge and S.[85] Based on the electronic structure, the introduction of Cl atoms may facilitate the formation of isolated [Ge_3S_9] group, which enlarges the band gap indirectly according to concept of "dimensional reduction".

Although the LDA method is suitable to describe the band structures and optical properties for most of NLO crystals according to the previous studies,[86] the energy band gap (~3.58 eV) for $NaBa_4Ge_3S_{10}Cl$ calculated by PBE0[87] (a senior exchange-correlation functional beyond LDA) is much better than that (~1.65 eV) by LDA, which is in a good agreement with the experiments (~3.49 eV). Accordingly, scissors-corrected LDA method is adopted to obtain the SHG[88] coefficients and further powder SHG (PSGH)[48] effect in $NaBa_4Ge_3S_{10}Cl$ and $AgGaS_2$ (as a comparison), which agree with the experimental measurements very well as listed in Table 3. Because the NLO response in $NaBa_4Ge_3S_{10}Cl$ and $AgGaS_2$ is determined by the [Ge_3S_9] and [GaS_4] anionic units respectively, their own SHG effect is approximately proportional with the density of [Ge_3S_9] or [GaS_4] in the unit cell, which may be roughly represented via the ratio of number of units in a unit cell/ cell volume,[89] i.e., the ratio between the SHG effect of $NaBa_4Ge_3S_{10}Cl$ and $AgGaS_2$ approximately equal $\frac{6/995.82}{4/341.02} \approx \frac{1}{2}$. However, the arrangement of [GeS_4] in [Ge_3S_9] ring is not totally parallel as the [GaS_4] case in $AgGaS_2$, thus, the SHG effect in $NaBa_4Ge_3S_{10}Cl$ decrease and the ratio between the SHG effect of $NaBa_4Ge_3S_{10}Cl$ and $AgGaS_2$ is actually down to about 1/3.

Conclusions

A new IR NLO chalcohalide, $NaBa_4Ge_3S_{10}Cl$, has been obtained. $NaBa_4Ge_3S_{10}Cl$ belongs to space group $P6_3$ and adopts a new structure type with the interesting $[Ge_3S_9]$ rings as the main structural units. The $[Ge_3S_9]$ rings are related via the 6_3 screw axis and linked by Na atoms to generate two-dimensional pseudo layers parallel to the *ab* plane. Although the $[Ge_3S_9]$ rings are parallelly aligned and should be beneficial to generate strong NLO response in a single pseudo layer, the orientations of the $[Ge_3S_9]$ rings are rotated by 60^o for two adjacent such pseudo layers and hence reduce the overall NLO properties. In addition the packing density of these rings is smaller than that in $AgGaS_2$. As a result, $NaBa_4Ge_3S_{10}Cl$ demonstrates only moderate NLO response about 1/3 that of $AgGaS_2$, but the value is still larger than most halides. If the macroscopic packing of the $[Ge_3S_9]$ rings or other similar NLO-active units could be optimized with higher density and parallel orientations in other chalcohalides, a much larger NLO response could be expected. Moreover, $NaBa_4Ge_3S_{10}Cl$ possesses large band gap of 3.49 eV, comparable to those of many NLO halides. Such large band gap may help to increase the laser damage threshold of the material and avoid the TPA problem of the conventional Nd: YAG 1064 nm laser. Considering these two aspects, although $NaBa_4Ge_3S_{10}Cl$ is still not "perfect", it already demonstrates that the chalcohalide can improve the property of halide NLO material by increasing their NLO response and that of chalcogenide NLO by increasing their band gap. Thus chalcohalides may provide a new design strategy for

IR NLO materials.by combining the large NLO response advantage of chalcogenide with large band gap advantage of halide.

Acknowledgements

This research was supported by the National Basic Research Project of China (No. 2010CB630701) and National Natural Science Foundation of China (No. 91122034 and No. 21271178).

References

1. C. Fischer and M. W. Sigrist, *Mid-IR difference frequency generation*, 2003.

2. S. Fossier, S. Salaun, J. Mangin, O. Bidault, I. Thenot, J. J. Zondy, W. D. Chen, F. Rotermund, V. Petrov, P. Petrov, J. Henningsen, A. Yelisseyev, L. Isaenko, S. Lobanov, O. Balachninaite, G. Slekys and V. Sirutkaitis, *J. Opt. Soc. Am. B*, 2004, **21**, 1981.

3. P. J. Kupecek, C. A. Schwartz and D. S. Chemla, *IEEE J. Quantum Elect.*, 1974, **QE10**, 540.

4. N. P. Barnes, D. J. Gettemy, J. R. Hietanen and R. A. Iannini, *Appl. Opt.*, 1989, **28**, 5162.

5. K. L. Vodopyanov, *J. Opt. Soc. Am. B*, 1993, **10**, 1723.

6. G. D. Boyd, E. Buehler and F. G. Storz, *Appl. Phys. Lett.*, 1971, **18**, 301.

7. G. C. Catella and D. Burlage, *MRS Bull.*, 1998, **23**, 28.

8. P. G. Schunemann, in *Perspectives on Inorganic, Organic, and Biological Crystal Growth: From Fundamentals to Applications*, eds. M. Skowronski, J. J. DeYoreo and C. A. Wang, 2007, vol. 916, pp. 541.

9. I. Chung, C. D. Malliakas, J. I. Jang, C. G. Canlas, D. P. Weliky and M. G. Kanatzidis, *J. Am. Chem. Soc.*, 2007, **129**, 14996.

10. T. K. Bera, J.-H. Song, A. J. Freeman, J. I. Jang, J. B. Ketterson and M. G. Kanatzidis, *Angew. Chem. Int. Ed.*, 2008, **47**, 7828.

11. T. K. Bera, J. I. Jang, J. B. Ketterson and M. G. Kanatzidis, *J. Am. Chem. Soc.*, 2009, **131**, 75.

12. I. Chung, J.-H. Song, J. I. Jang, A. J. Freeman, J. B. Ketterson and M. G. Kanatzidis, *J. Am. Chem. Soc.*, 2009, **131**, 2647.

13. M.-C. Chen, L.-H. Li, Y.-B. Chen and L. Chen, *J. Am. Chem. Soc.*, 2011, **133**, 4617.

14. J. Zhang, Z. Zhang, Y. Sun, C. Zhang, S. Zhang, Y. Liu and X. Tao, *J. Mater. Chem.*, 2012, **22**, 9921.

15. K. Feng, X. Jiang, L. Kang, W. Yin, W. Hao, Z. Lin, J. Yao, Y. Wu and C. Chen, *Dalton Trans.*, 2013, **42**, 13635.

16. L. Kang, D. M. Ramo, Z. Lin, P. D. Bristowe, J. Qin and C. Chen, *J. Mater. Chem. C*, 2013, **1**, 7363.

17. S.-M. Kuo, Y.-M. Chang, I. Chung, J.-I. Jang, B.-H. Her, S.-H. Yang, J. B. Ketterson, M. G. Kanatzidis and K.-F. Hsu, *Chem. Mater.*, 2013, **25**, 2427.

18. M. Zhang, S. Pan, Z. Yang, Y. Wang, X. Su, Y. Yang, Z. Huang, S. Han and K. R. Poeppelmeier, *J. Mater. Chem. C*, 2013, **1**, 4740.

19. M.-J. Zhang, X.-M. Jiang, L.-J. Zhou and G.-C. Guo, *J. Mater. Chem. C*, 2013,

1, 4754.

20. G. M. H. Knippels, A. F. G. van der Meer, A. M. MacLeod, A. Yelisseyev, L. Isaenko, S. Lobanov, I. Thenot and J. J. Zondy, *Opt. Lett.*, 2001, **26**, 617.

21. V. V. Badikov, V. I. Chizhikov, V. V. Efimenko, T. D. Efimenko, V. L. Panyutin, G. S. Shevyrdyaeva and S. I. Scherbakov, *Opt. Mater.*, 2003, **23**, 575.

22. V. Petrov, A. Yelisseyev, L. Isaenko, S. Lobanov, A. Titov and J. J. Zondy, *Appl. Phys. B*, 2004, **78**, 543.

23. X. Lin, G. Zhang and N. Ye, *Cryst. Growth Des.*, 2009, **9**, 1186.

24. J. Yao, D. Mei, L. Bai, Z. Lin, W. Yin, P. Fu and Y. Wu, *Inorg. Chem.*, 2010, **49**, 9212.

25. J. Yao, W. Yin, K. Feng, X. Li, D. Mei, Q. Lu, Y. Ni, Z. Zhang, Z. Hu and Y. Wu, *J. Cryst. Growth*, 2012, **346**, 1.

26. Y. Kim, I.-S. Seo, S. W. Martin, J. Baek, P. S. Halasyamani, N. Arumugam and H. Steinfink, *Chem. Mater.*, 2008, **20**, 6048.

27. D. Mei, W. Yin, K. Feng, Z. Lin, L. Bai, J. Yao and Y. Wu, *Inorg. Chem.*, 2012, **51**, 1035.

28. W. Yin, K. Feng, W. Hao, J. Yao and Y. Wu, *Inorg. Chem.*, 2012, **51**, 5839.

29. W. Yin, K. Feng, R. He, D. Mei, Z. Lin, J. Yao and Y. Wu, *Dalton Trans.*, 2012, **41**, 5653.

30. J. Zhang, N. B. Su, C. L. Yang, J. G. Qin, N. Ye, B. C. Wu and C. T. Chen, in *Electro-Optic and Second Harmonic Generation Materials, Devices, and Applications Ii*, ed. C. Chen, 1998, vol. 3556, pp. 1.

31. L. C. Tang, J. Y. Huang, C. S. Chang, M. H. Lee and L. Q. Liu, *J. Phys.: Condens. Matter*, 2005, **17**, 7275.

32. G. Zhang, T. Liu, T. Zhu, J. Qin, Y. Wu and C. Chen, *Opt. Mater.*, 2008, **31**, 110.

33. G. Zhang, J. Qin, T. Liu, T. Zhu, P. Fu, Y. Wu and C. Chen, *Cryst. Growth Des.*, 2008, **8**, 2946.

34. T. Liu, J. Qin, G. Zhang, T. Zhu, F. Niu, Y. Wu and C. Chen, *Appl. Phys. Lett.*, 2008, **93**.

35. G. Zhang, J. Qin, T. Liu, Y. Li, Y. Wu and C. Chen, *Appl. Phys. Lett.*, 2009, **95**.

36. Y. Kamihara, H. Hiramatsu, M. Hirano, R. Kawamura, H. Yanagi, T. Kamiya and H. Hosono, *J. Am. Chem. Soc.*, 2006, **128**, 10012.

37. X. H. Chen, T. Wu, G. Wu, R. H. Liu, H. Chen and D. F. Fang, *Nature*, 2008, **453**, 761.

38. C. de la Cruz, Q. Huang, J. W. Lynn, J. Li, W. Ratcliff, II, J. L. Zarestky, H. A. Mook, G. F. Chen, J. L. Luo, N. L. Wang and P. Dai, *Nature*, 2008, **453**, 899.

39. H. Hiramatsu, H. Kamioka, K. Ueda, H. Ohta, T. Kamiya, M. Hirano and H.

Hosono, *Phys. Status Solidi A*, 2006, **203**, 2800.

40. R. L. Gitzendanner and F. J. DiSalvo, *Inorg. Chem.*, 1996, **35**, 2623.

41. S.-P. Guo, G.-C. Guo, M.-S. Wang, J.-P. Zou, H.-Y. Zeng, L.-Z. Cai and J.-S. Huang, *Chem. Commun.*, 2009, 4366.

42. X.-M. Jiang, M.-J. Zhang, H.-Y. Zeng, G.-C. Guo and J.-S. Huang, *J. Am. Chem. Soc.*, 2011, **133**, 3410.

43. A. H. Reshak, H. Kamarudin, S. Auluck and I. V. Kityk, *J. Phys. Chem. B*, 2011, **115**, 11763.

44. P. Yu, L.-J. Zhou and L. Chen, *J. Am. Chem. Soc.*, 2012, **134**, 2227.

45. J. Rigaku Corporation: Tokyo, *CrystalClear*, 2008.

46. G. M. Sheldrick, *Acta Crystallogr., Sect. A: Found. Crystallogr.*, 2008, **64**, 112.

47. L. M. Gelato and E. Parthe, *J Appl Crystallogr*, 1987, **20**, 139.

48. S. K. Kurtz and T. T. Perry, *J. Appl. Phys.*, 1968, **39**, 3798.

49. M. C. Payne, M. P. Teter, D. C. Allan, T. A. Arias and J. D. Joannopoulos, *Rev. Mod. Phys.*, 1992, **64**, 1045.

50. S. J. Clark, M. D. Segall, C. J. Pickard, P. J. Hasnip, M. J. Probert, K. Refson and M. C. Payne, *Z. Kristallogr.*, 2005, **220**, 567.

51. W. Kohn and L. J. Sham, *Phys. Rev.*, 1965, **140**, 1133.

52. J. S. Lin, A. Qteish, M. C. Payne and V. Heine, *Phys. Rev. B*, 1993, **47**, 4174.

53. L. Kleinman and D. M. Bylander, *Phys. Rev. Lett.*, 1982, **48**, 1425.

54. H. J. Monkhorst and J. D. Pack, *Phys. Rev. B*, 1976, **13**, 5188.

55. E. Levi, G. Gershinsky, D. Aurbach and O. Isnard, *Inorg. Chem.*, 2009, **48**, 8751.

56. D. J. Hinz, G. Meyer, T. Dedecke and W. Urland, *Angew. Chem. Int. Ed.*, 1995, **34**, 71.

57. V. L. Cherginets, V. N. Baumer, S. S. Galkin, L. V. Glushkova, T. P. Rebrova and Z. V. Shtitelman, *Inorg. Chem.*, 2006, **45**, 7367.

58. W. Yin, K. Feng, D. Mei, J. Yao, P. Fu and Y. Wu, *Dalton Trans.*, 2012, **41**, 2272.

59. K. Feng, Y. Shi, W. Yin, W. Wang, J. Yao and Y. Wu, *Inorg. Chem.*, 2012, **51**, 11144.

60. G. Meyer and S. Masselmann, *Chem. Mater.*, 1998, **10**, 2994.

61. M. S. Wickleder, P. Egger, T. Riedener, N. Furer, H. U. Gudel and J. Hulliger, *Chem. Mater.*, 1996, **8**, 2828.

62. G. Bugli, D. Carre and S. Barnier, *Acta Crystallogr., Sect. B: Struct. Sci*, 1978, **34**, 3186.

63. G. Eulenberger, *Z. Kristallogr.*, 1977, **145**, 427.

64. K. O. Klepp and F. Fabian, *Z. Naturforsch., B: Chem. Sci.*, 1999, **54**, 1499.

65. Y. Dong, J. Do and H. Yun, *Z. Anorg. Allg. Chem.*, 2009, **635**, 2676.

66. J. C. Jumas, Olivierf.J, Vermotga.F, M. Ribes, Philippo.E and M. Maurin, *Rev. Chim. Miner.*, 1974, **11**, 13.

67. E. Philippo, M. Ribes and O. Lindqvis, *Rev. Chim. Miner.*, 1971, **8**, 477.

68. J. Olivier Fourcade, E. Philippot, M. Ribes and M. Maurin, *Comptes Rendus Hebdomadaires des Seances de l`Academie des Sciences, Serie C, Sciences Chimiques*, 1972, 1185.

69. C. Chen, *Scientia Sinica*, 1979, **22**, 756.

70. C. T. Chen and G. Z. Liu, *Annual Review of Materials Science*, 1986, **16**, 203.

71. C. T. Chen, Y. C. Wu and R. K. Li, *International Reviews in Physical Chemistry*, 1989, **8**, 65.

72. Z. G. Hu, T. Higashiyama, M. Yoshimura, Y. K. Yap, Y. Mori and T. Sasaki, *Jpn. J. Appl. Phys.*, 1998, **37**, L1093.

73. N. Ye, W. R. Zeng, J. Jiang, B. C. Wu, C. T. Chen, B. H. Feng and X. L. Zhang, *J. Opt. Soc. Am. B*, 2000, **17**, 764.

74. I. Shoji, H. Nakamura, K. Ohdaira, T. Kondo, R. Ito, T. Okamoto, K. Tatsuki and S. Kubota, *J. Opt. Soc. Am. B*, 1999, **16**, 620.

75. D. A. Roberts, *Quantum Electronics, IEEE Journal of*, 1992, **28**, 2057.

76. O. Schevciw and W. B. White, *Mater. Res. Bull.*, 1983, **18**, 1059.

77. E. A. Axtell, J. H. Liao, Z. Pikramenou and M. G. Kanatzidis, *Chem.-Eur. J.*, 1996, **2**, 656.

78. E. A. Axtell, Y. Park, K. Chondroudis and M. G. Kanatzidis, *J. Am. Chem. Soc.*, 1998, **120**, 124.

79. L. Wang and S.-J. Hwu, *Chem. Mater.*, 2007, **19**, 6212.

80. J. Androulakis, S. C. Peter, H. Li, C. D. Malliakas, J. A. Peters, Z. Liu, B. W. Wessels, J.-H. Song, H. Jin, A. J. Freeman and M. G. Kanatzidis, *Adv. Mater.*, 2011, **23**, 4163.

81. S. Johnsen, S. C. Peter, S. L. Nguyen, J.-H. Song, H. Jin, A. J. Freeman and M. G. Kanatzidis, *Chem. Mater.*, 2011, **23**, 4375.

82. K. Feng, W. Yin, Z. Lin, J. Yao and Y. Wu, *Inorg. Chem.*, 2013, **52**, 11503.

83. D. M. Ceperley and B. J. Alder, *Phys. Rev. Lett.*, 1980, **45**, 566.

84. M.-H. Lee, C.-H. Yang and J.-H. Jan, *Phys. Rev. B*, 2004, **70**, 235110.

85. C. T. Chen, T. Sasaki, R. K. Li, Y. C. Wu, Z. S. Lin, Y. Mori, Z. G. Hu, J. Y. Wang, S. Uda, M. Yoshimura and Y. Kaneda, *Nonlinear optical borate crystals*, Wiley-VCH press, Germany, 2012.

86. Z. S. LIN, L. KANG, T. ZHENG, R. HE, H. HUANG, CHEN and C. T., *Strategy for the optical property studies in ultraviolet nonlinear optical*

crystals from density functional theory, Elsevier, Amsterdam, PAYS-BAS, 2012.

87. C. Adamo and V. Barone, *Chem. Phys. Lett.*, 1998, **298**, 113.

88. J. Lin, Z. P. Liu, C. T. Chen and M. H. Lee, *Phys. Rev. B-Condensed Matter*, 1999, **60**, 13380.

89. C. Chen, Z. Lin and Z. Wang, *Appl Phys B*, 2005, **80**, 1.

90. L. Bai, Z. S. Lin, Z. Z. Wang, C. T. Chen and M. H. Lee, *J. Chem. Phys.*, 2004, **120**, 8772.

Figure Captions

Figure 1 Experimental (red) and simulated (black) x–ray powder diffraction data of $NaBa_4Ge_3S_{10}Cl$

Figure 2 Crystal structure of $NaBa_4Ge_3S_{10}Cl$ viewed down [110] direction

Figure 3 The $[Ge_3S_9]$ pseudo-layer (A) and the chain structure (B) in $NaBa_4Ge_3S_{10}Cl$

Figure 4 The coordination environments of cations in $NaBa_4Ge_3S_{10}Cl$

Figure 5 Diffuse reflectance spectrum of $NaBa_4Ge_3S_{10}Cl$

Figure 6 Band structure PDOS projected on all atoms (A) and DOS (B) in $NaBa_4Ge_3S_{10}Cl$

Table 1 Crystal data and structure refinements for $NaBa_4Ge_3S_{10}Cl$

	$NaBa_4Ge_3S_{10}Cl$
Fw	1146.17
a(Å)	9.7653(2)
c(Å)	12.0581(3)
Space group	$P6_3$
V(Å^3)	995.82(6)
Z	2
T(K)	293(2)
λ (Å)	0.71073
ρ_c(g/cm^3)	3.823
μ(cm^{-1})	13.427
R(F) [a]	0.0424
$R_W(F_o^2)$ [b]	0.1245
Flack parameter	0.06(4)

[a] $R(F) = \sum \| \| F_o \square - \square F_c \| \| / \sum | F_o \square$ for $F_o^2 > 2\sigma(F_o^2)$.

[b] $R_w(F_o^2) = \{\sum [w(F_o^2 - F_c^2)^2] / \sum w F_o^4\}^{1/2}$ for all data. $w^{-1} = \sigma^2(F_o^2) + (zP)^2$, where $P =$

$(\mathrm{Max}(F_o^2, 0) + 2\,F_c^2)/3$.

Table 2 Selected bond lengths (Å) and bond angles (°) for $NaBa_4Ge_3S_{10}Cl$

Ba1–S4	2.991 (2)	Ba2–S2×3	3.146 (3)
Ba1–Cl1	2.994 (1)	Ba2–S3×3	3.182 (3)
Ba1–S3	3.204 (4)	Na–S3×3	2.820 (3)
Ba1–S2	3.346 (3)	Na–Cl1	3.004 (17)
Ba1–S1	3.380 (4)	Na–Cl1	3.025 (17)
Ba1–S2	3.474 (4)	Ge–S2	2.149 (4)
Ba1–S3	3.550 (4)	Ge–S3	2.171 (3)
Ba1–S2	3.561 (4)	Ge–S1	2.259 (3)
Ba2–S4	3.084 (7)	Ge–S1	2.265 (3)

Table 3 The calculated SHG/PSHG results of $NaBa_4Ge_3S_{10}Cl$ and $AgGaS_2$ (as a comparison)

	Cal. by scissors-corrected LDA (pm/V)	
	SHG	PSHG
$NaBa_4Ge_3S_{10}Cl$	$d_{15} = d_{24} = -2.72$; $d_{33} = 6.81$	3.44
$AgGaS_2$	$d_{36} = 14.1$[90]	11.92

Figure 1

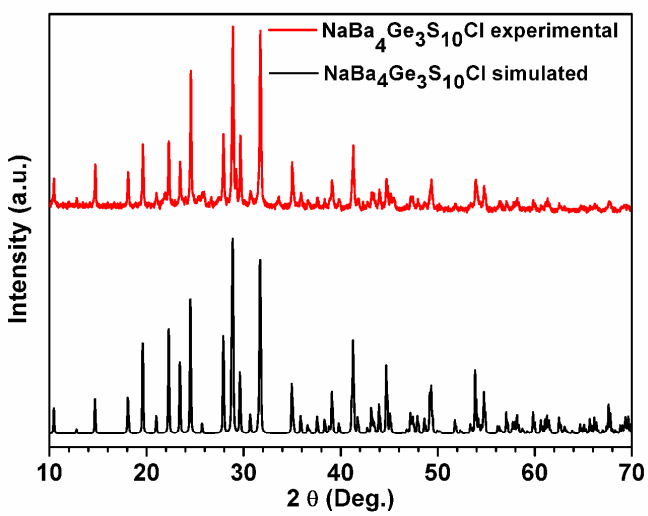

Figure 2

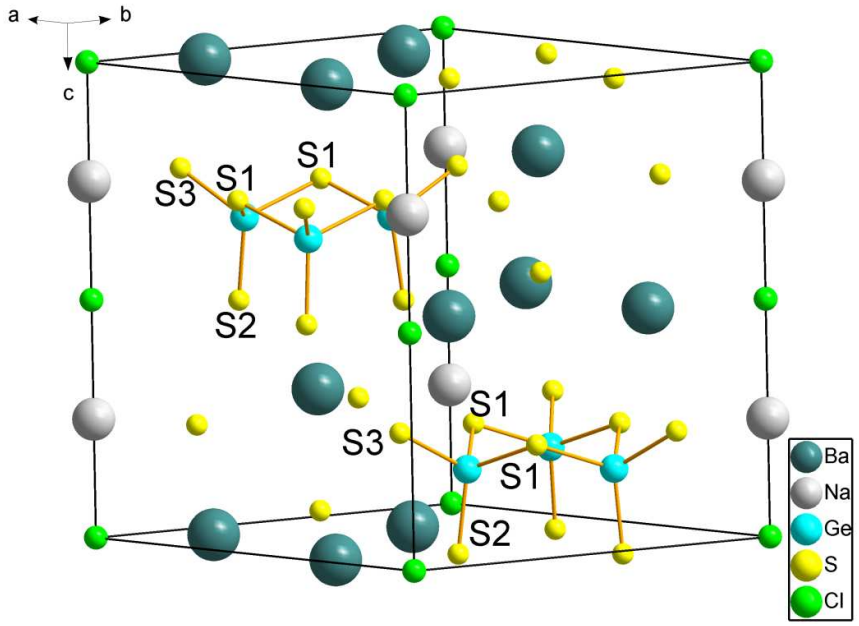

Figure 3

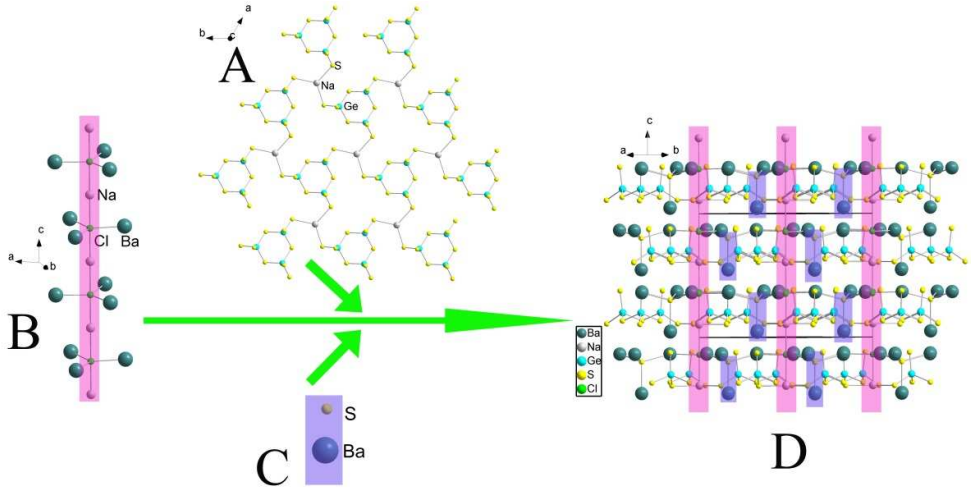

Figure 4

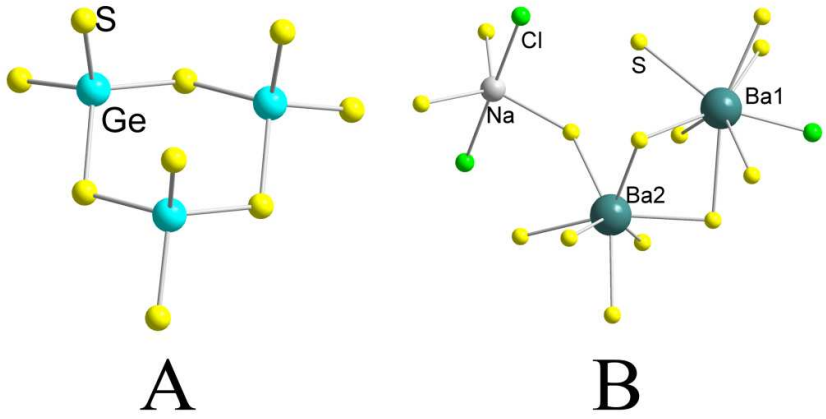

Figure 5

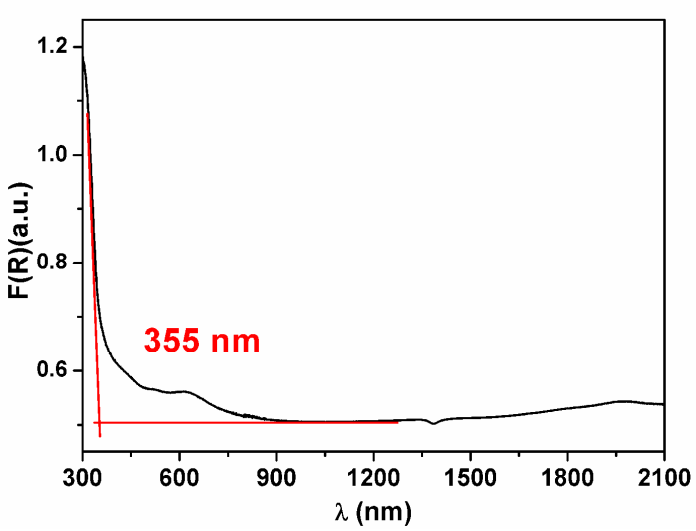

Figure 6

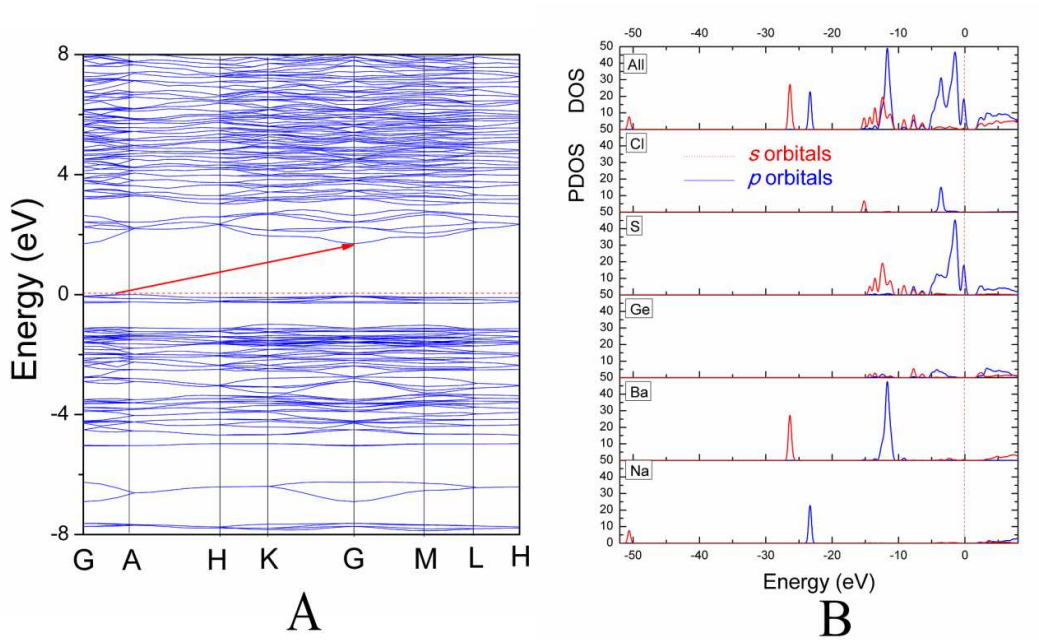

Table of Contents Entry

Large band gap and moderate NLO response was found in a new IR NLO chalcohalide, $NaBa_4Ge_3S_{10}Cl$.